

EFFECT OF CYLINDER LOCATION INSIDE A RECTANGULAR DUCT ON THE EXCITATION MECHANISM OF ACOUSTIC RESONANCE

N. Arafa¹, A. Tariq¹, A. Mohany¹, M. Hassan²

¹ AeroAcoustics and Noise Control Laboratory, Faculty of Engineering and Applied Science, University of Ontario Institute of Technology, Oshawa, ON, Canada.

² Fluid-Structure Interaction Laboratory, School of Engineering, University of Guelph, Guelph, ON, Canada.

ABSTRACT

The flow-sound interaction mechanism of a single cylinder in cross-flow is investigated experimentally. The cylinder is located at different vertical locations inside a rectangular duct in order to investigate the effect of the cylinder location on the excitation mechanism of acoustic resonance. During the tests, the acoustic cross-modes of the duct housing the cylinder are self-excited. It is found that the cylinder location affects the process of the flow-excited acoustic resonance and the levels of the generated acoustic pressure. The resonance of a specific acoustic cross-mode is excited when the cylinder is located at its acoustic pressure node, which is the acoustic particle velocity anti-node. However, when the cylinder is shifted away from the pressure node of a certain acoustic cross-mode, a combination of cross-modes is excited and their intensity seems to be proportional to the ratio of the acoustic particle velocities of these modes at the cylinder's location. Moreover, as the cylinder moves closer to the top wall (or the bottom wall) of the rectangular duct, the Strouhal number value decreases due to the interference between the wake of the cylinder and the duct wall. Therefore, the onset of acoustic resonance for this case occurs at a higher value of reduced flow velocity.

RÉSUMÉ

Le mécanisme d'interaction d'un seul cylindre soumis à un écoulement transverse est étudié expérimentalement. Le cylindre est placé à des endroits différents dans un conduit rectangulaire afin de découvrir les effets de l'emplacement du cylindre sur le mécanisme d'excitation de résonance acoustique. Pendant les tests, les modes transversaux du conduit sont auto-excités. Les résultats montrent que le phénomène de résonance acoustique excitée par l'écoulement ainsi que le niveau de pression acoustique sont affectés par l'emplacement du cylindre. La résonance d'un certain mode acoustique transversal est excitée quand le cylindre se situe au nœud de pression acoustique, ce qui est également l'anti-nœud de vitesse de particule acoustique. Néanmoins, lorsque le cylindre est décalé loin du nœud de pression d'un certain mode acoustique transversal, une combinaison de mode transversaux est excitée et leur intensité semble être proportionnelle au rapport entre la vitesse de particule acoustique de ces modes à l'emplacement du cylindre. De plus, le nombre de Strouhal diminue si le cylindre approche la paroi du conduit paroi du haut ou du bas à cause de l'interférence entre le sillage du cylindre et la paroi du conduit. Par conséquent, le début de la résonance acoustique pour ce cas a lieu à une valeur plus élevée de la vitesse réduite de l'écoulement.

1. INTRODUCTION

The aeroacoustic sound or 'Aeolian tones' was first observed by Strouhal in 1878. The phenomenon was attributed to the friction between the air stream and any moving body and thus referred to by a 'friction tone' [1]. Subsequently, this phenomenon became of interest for many researchers, (e.g. Rayleigh [2], Bernard [3], and Relf [4]) who concluded that the sound is actually a result of the periodic vortex shedding behind any bluff body [5]. For a bluff body contained inside a duct, when the vortex shedding frequency coincides with one of the acoustic natural frequencies of the duct, a

feedback cycle may occur where the vortex shedding acts as a sound source and excites an acoustic standing wave which, in turn, enhances the shedding process and thereby creates a strong acoustic resonance. This process is known as the flow-excited acoustic resonance and it often leads to the generation of acute noise problems and/or excessive vibrations [6]. Since the acoustic resonance phenomenon is not yet fully understood, it can be dangerously unpredictable and may cause catastrophic failures in many applications such as power generation and transport. Acoustic resonance in tube bundles of heat exchangers has received a considerable amount of attention over the

past few decades because of its relevance to many industrial applications (e.g. Blevins and Bressler [7], Ziada et al. [8], Ziada and Oengoren [9, 10], Oengoren and Ziada [11], Eisinger et al. [12], Eisinger and Sullivan [13], and Feenstra et al. [14]). Nevertheless, the excitation mechanisms of acoustic resonance are still not fully understood. The primary reason for this is that most of the previous studies were directed toward finding solutions to specific existing problems rather than understanding the underlying physics of these excitation mechanisms, as discussed in detail by Weaver [15]. Several techniques have been suggested to suppress the acoustic resonance in tube bundles. One of these techniques is to change the frequency of the excited acoustic mode of the system by placing baffles in the tube bundle. Basically, this technique shifts the acoustic resonance frequency above the vortex shedding frequency and therefore the acoustic resonance would not occur at a specific range of flow velocities. However, this technique is not effective to suppress the higher acoustic modes [16]. Zdravkovich and Nuttall [17] investigated the suppression of the acoustic resonance in staggered tube arrays by eliminating different cylinders from specific locations inside the tube bundle. They have found that the removal of any of the cylinders that are located in the first row would eliminate the acoustic resonance. However, for the second row, only removal of the cylinders that are located at the acoustic pressure node of a certain cross-mode would be effective to suppress the acoustic resonance. Furthermore, for the third row, the removal of any cylinder did not suppress the acoustic resonance even when the cylinders located at the acoustic pressure node were removed. These results are quite surprising and thus, the relationship between the cylinder location inside a tube bundle and the acoustic resonance mechanism needs to be further investigated. Therefore, the main objective of this work is to investigate the flow-sound interaction mechanism of single cylinder located at different locations inside a rectangular duct and subjected to cross-flow. The outcome of this work shall clarify how the tubes located away from the location of the maximum acoustic particle velocity contribute to the excitation mechanism of acoustic resonance.

2. ACOUSTIC CROSS-MODES IN A DUCT

The acoustic cross-modes of a duct are the modes that excite acoustic standing wave inside the duct that oscillate in a direction perpendicular to both the cylinder axis and the main flow velocity. These acoustic cross-modes oscillate with a simple harmonic motion in time [18]. The frequencies of these cross-modes are given by:

$$f_{a,n} = n \frac{c}{2h}, \quad n = 1, 2, 3, \dots \quad (1)$$

where f_a is the natural frequency of a certain acoustic mode, n is an index that indicates the order of this mode, c is the speed of sound, and h is the duct height. Figure (1) shows the distribution of both the acoustic pressure and the acoustic particle velocity along the duct height for the first three cross-modes. The acoustic pressure for the build-up standing wave follows a sinusoidal distribution along the duct height. The acoustic particle velocity will also take a similar sinusoidal distribution with 90° phase shift. The acoustic pressure field inside the duct for the first acoustic cross-mode is simulated and shown in Figure (2). The resonant fields in the duct housing the cylinder are obtained using finite-element analysis (FEA) in ABAQUS. The acoustic pressure of the resonant mode can be expressed as:

$$p = \varphi e^{i(2\pi f)t} \quad (2)$$

where φ is a variable that satisfies the following Helmholtz equation:

$$\nabla^2 \varphi + k^2 \varphi = 0 \quad (3)$$

where k is the wave number ($k = 2\pi f_a / c$) and c is the speed of sound. At the inlet and the outlet section of the duct, the boundary condition for the lowest acoustic modes is approximately zero acoustic pressure. More details about the simulation technique can be found in Mohany and Ziada [19]. It is observed from Figure (2) that the cylinder is located at the acoustic pressure node for the first cross-mode. The relation between the cylinder location and the pressure node of each cross-mode will dictate the excitation mechanism, which is discussed in detail in the results section.

3. VORTEX SHEDDING FREQUENCY

The value of the vortex shedding frequency behind a circular cylinder depends on the flow velocity and cylinder's diameter. The vortex shedding frequency is given by:

$$f_v = \frac{St U}{D} \quad (4)$$

where f_v is the vortex shedding frequency, St is the Strouhal Number, U is the flow velocity, D is the diameter of the cylinder. For a single cylinder, the Strouhal number has a constant value around 0.2 over a wide range of Reynolds numbers [20]. This indicates that the relationship between the flow velocity and the vortex shedding frequency will be linear. The flow-excited acoustic resonance will occur upon the coincidence of the vortex shedding frequency with one of the acoustic cross-modes frequencies of the duct,

provided that the excitation energy of the flow is high enough to overcome the acoustic damping of the system.

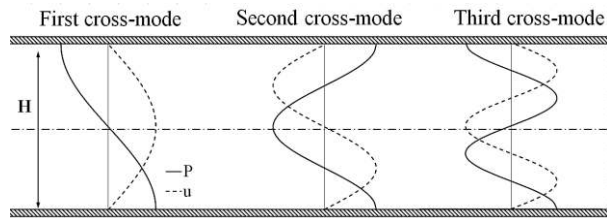


Figure 1: Normalized acoustic pressure and acoustic particle velocity distribution along the duct height (H).

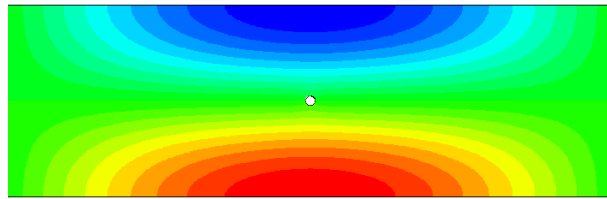


Figure 2: Acoustic pressure field inside the duct housing the cylinder for the first cross-mode. The cylinder is located in the middle of the duct height.

4. EXPERIMENTAL SETUP

An experimental set-up was designed specifically for this work, which is conducive to self-generation of acoustic resonance for the first three acoustic cross-modes of the duct housing the cylinder. The experimental setup consists of an open loop wind tunnel connected to a centrifugal air blower that is driven by an electrical motor with a variable frequency drive to control the air velocity inside the duct, as shown schematically in Figure (3). The test section height is 254 mm and the width is 127 mm. The test section is connected to a single-sided diffuser with an inclusion angle of 14° and both of them are manufactured out of plywood with 19 mm thickness. The diffuser is connected to the blower via a flexible connection in order to reduce any vibration transmission to the test section. The maximum flow velocity achievable in this

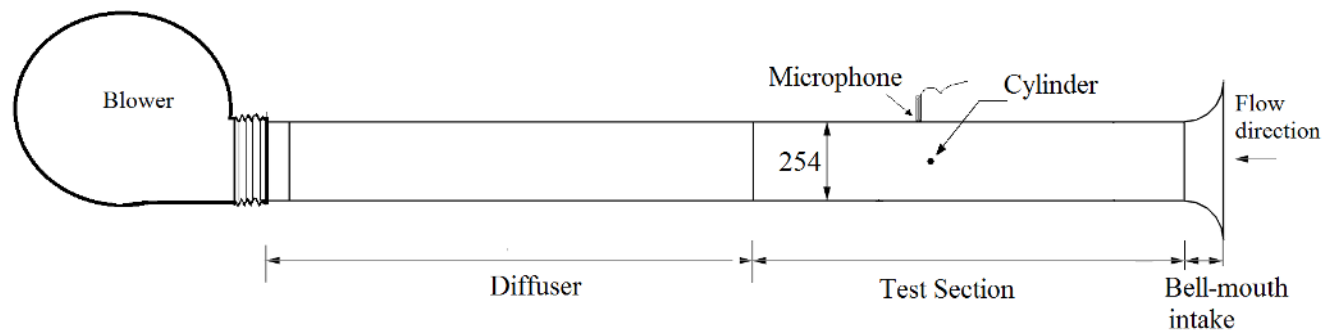


Figure 3: Schematic drawing of the experimental setup, all dimensions are in millimeters.

test section is 160 m/s. The tested cylinder is rigidly mounted between the walls of the test section at various heights and subjected to cross-flow air stream. The aeroacoustic response is measured for each position by a pressure-field microphone. Figure (4) shows the microphone position with respect to the cylinder's location. The microphone is located at the position of the maximum acoustic pressure, which was determined in a separate experiment as shown in Figure (5).

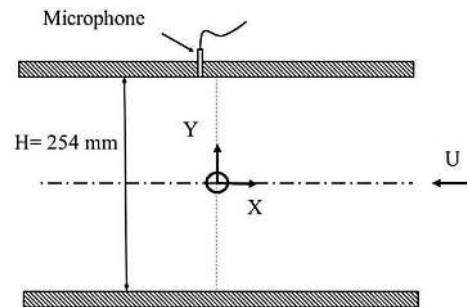


Figure 4: Schematic side view of the test section showing the coordinates system, the cylinder is positioned at $Y/H=0$ and $X/H=0$, the microphone is flush-mounted on the top wall at $X/H=-0.1$.

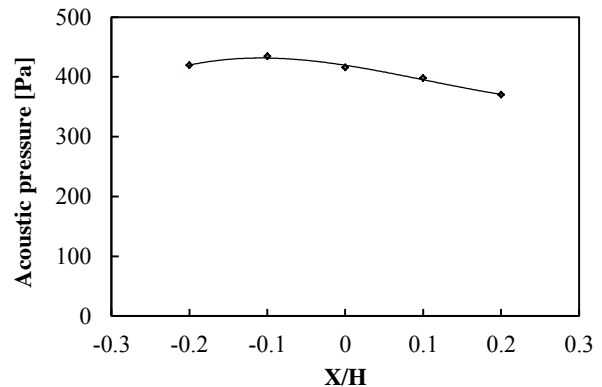


Figure 5: Peaks of the acoustic pressure of the first cross-mode versus the microphone positions for a single cylinder, $D=19$ mm and $U=70.3$ m/s. The cylinder is located at $Y/H=0$ and $X/H=0$. Negative values represent the downstream direction.

In that experiment, the microphone was flush-mounted at the top wall of the test section and moved to several stream-wise locations, with respect to the cylinder, in order to determine the location of the maximum acoustic pressure when a specific acoustic resonance mode is excited. The microphone signal is recorded with a data acquisition card (National Instruments, model number: PCI-6035E) and a LabView program is used for spectral analysis. Each spectrum is obtained by averaging 100 samples and the data is collected at a sampling rate of 10 kHz.

5. RESULTS

The aeroacoustic response of the cylinder is obtained by performing spectral analysis for the measured acoustic pressure. Figure (6) shows a waterfall plot of the acoustic pressure spectra for a cylinder positioned in the middle of the duct height, $Y/H=0$, while Figure (7) shows the aeroacoustic response for the same case. Figure (7) is extracted from the waterfall plot of the acoustic pressure spectra where each point represents the amplitude and frequency of the vortex shedding component taken from the pressure spectrum at each flow velocity. Since the values of the vortex shedding frequency depend on the cylinder's diameter as shown in Eqn. (4), the frequency coincidence will occur over different velocity range depending on the cylinder's diameter. Thus, the reduced velocity, U_r , will be used to represent the flow velocity. The reduced velocity is given by:

$$U_r = \frac{U}{f_a D} \quad (5)$$

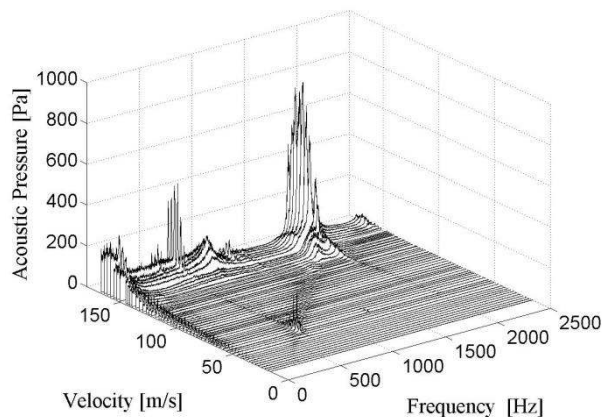


Figure 6: Waterfall plot of the pressure spectra for a cylinder positioned at $Y/H=0$, $D=15.7$ mm.

Figure (7) shows that the frequency of the vortex shedding progresses with the flow velocity following a linear relationship with an average Strouhal number of 0.196. When the value of the vortex shedding frequency coincides with the frequency of the first acoustic cross-

mode, acute acoustic pressure is generated. Moreover, the frequency is retrained at the value of the first acoustic cross-mode over a certain range of velocities, which is referred to by the *lock-in* region. As the flow velocity increases, the vortex-shedding frequency exits the lock-in region and follows the same linear relationship until reaching the frequency of the third acoustic cross-mode, where another lock-in region is obtained and severe noise is generated. The second acoustic cross-mode is not excited in this case as the cylinder is located at its acoustic pressure anti-node, which is an acoustic particle velocity node, as shown in Figure (1). Figure (8) shows a waterfall plot of the acoustic pressure spectra for a cylinder positioned at 63.5 mm away from the duct's centerline, i.e. $Y/H=0.25$, while Figure (9) shows the aeroacoustic response for the same case.

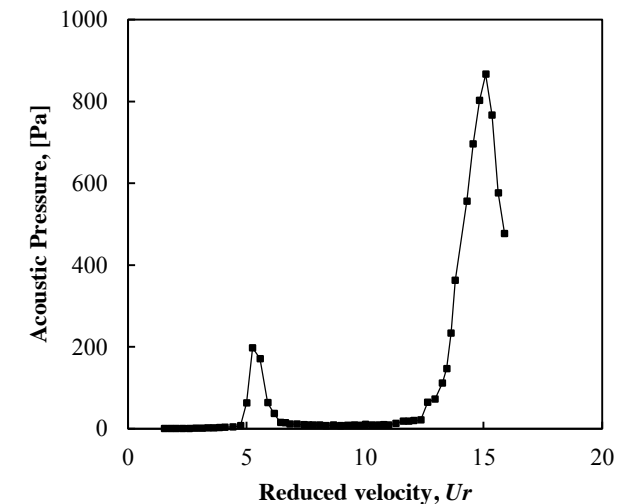
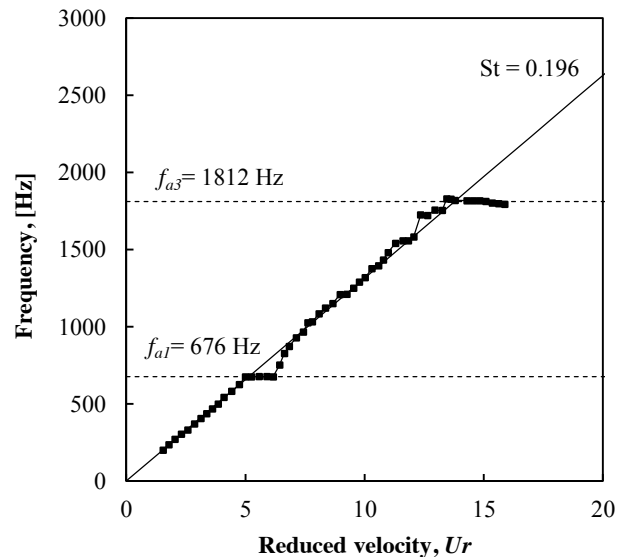


Figure 7: Aeroacoustic response of a single cylinder in cross-flow positioned at $Y/H=0$, $D=15.7$ mm.

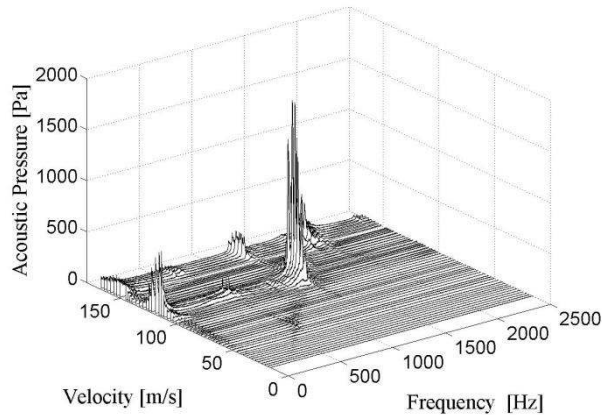


Figure 8: Waterfall plot of the pressure spectra for a cylinder positioned at $Y/H=0.25$, $D= 15.7$ mm.

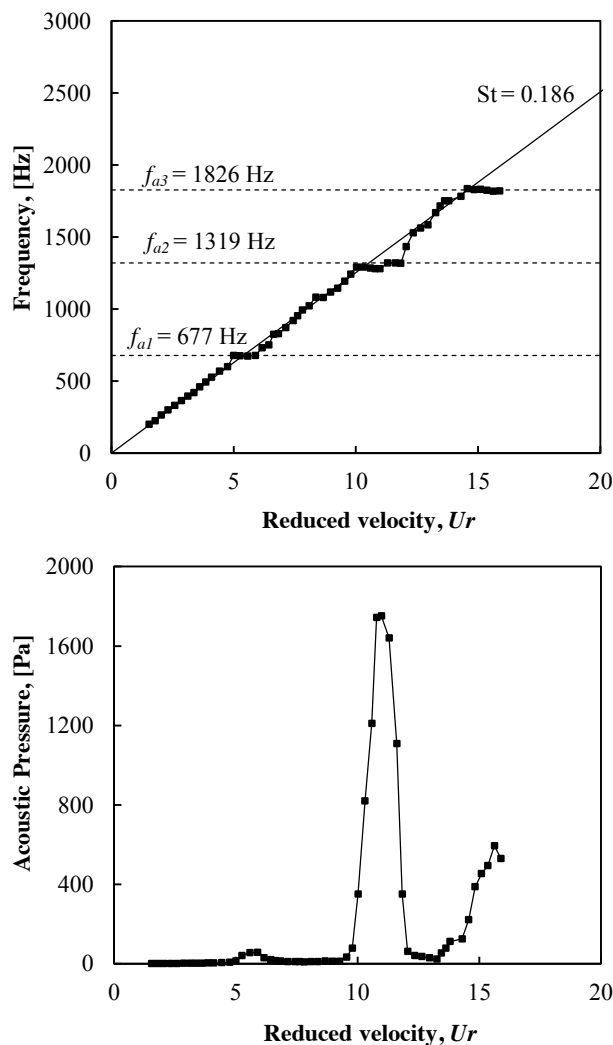


Figure 9: Aeroacoustic response of single cylinder in cross-flow positioned at $Y/H=0.25$, $D= 15.7$ mm.

It is clear from Figure (9) that the second acoustic cross-mode excitation is dominant as the cylinder is located at its acoustic pressure node. However, the first and the third cross-modes are also excited in this case as the cylinder is not located at any of their acoustic pressure anti-nodes. The generated acoustic pressure depends on the dynamic head of the flow and thus, on the flow velocity. As mentioned before, the velocity of frequency coincidence depends on the cylinder diameter. This indicates that different levels of acoustic pressures will be obtained when using different cylinder diameters. Thus, the logarithmic sound pressure level (SPL) will be used to represent the acoustic pressure in order to compare the results. The sound pressure level (in dB) is calculated by:

$$SPL = 20 \log \left(\frac{P_{rms}}{P_{ref}} \right) \quad (6)$$

Where P_{rms} is the root mean square value of the acoustic pressure and P_{ref} is a reference pressure value that equals to $20 \mu\text{Pa}$.

Figure (10) shows a comparison of the sound pressure levels for a single cylinder with a diameter of 12.7 mm, at several vertical locations inside the duct. Figure (11) shows the same comparison for another cylinder with a diameter of 15.7 mm, at the same vertical locations. It is observed that when the cylinder is located in the middle of the duct height, i.e. $Y/H=0$, the excitation of the first and the third acoustic cross-modes is the highest among the other locations. This is due to the fact that this location is the acoustic particle velocity anti-node for both the first and the third acoustic cross-modes; refer to Figure (1). Moreover, it is clear from Figure (10) that as the cylinder moves away from the duct centerline, the excitation levels of the first and the third acoustic cross-modes around reduced velocity values of 5 and 15, respectively, decreases. It is also observed that as the cylinder approaches $Y/H = 0.25$, which is the acoustic particle velocity anti-node of the second mode, the level of excitation of the second cross-mode increases. Yet, this level decreases as the cylinder moves beyond the acoustic pressure node, i.e. at $Y/H = 0.375$. Similar results are observed for another single cylinder with a diameter of 15.7 mm, as shown in Figure (11), which indicates that this behaviour is independent of the cylinder diameter.

It is clear from Figures (10) and (11) that the level of the excited acoustic pressure for each acoustic cross-mode varies depending on the cylinder's location. Since the acoustic resonance mechanism seems to be triggered by the acoustic particle velocity at the cylinder's location, it is interesting to determine if the

levels of the excited acoustic pressure at different cylinder locations are proportional to the normalized acoustic particle velocity distribution for each cross-mode. Figure (12) shows the ratio of the acoustic particle velocity at the cylinder's location to the maximum acoustic particle velocity for each cross-mode. This ratio is equal to the ratio of the acoustic pressure excited at a specific cylinder's location to the maximum acoustic pressure obtained when the cylinder is located at the acoustic pressure node of a certain cross-mode.

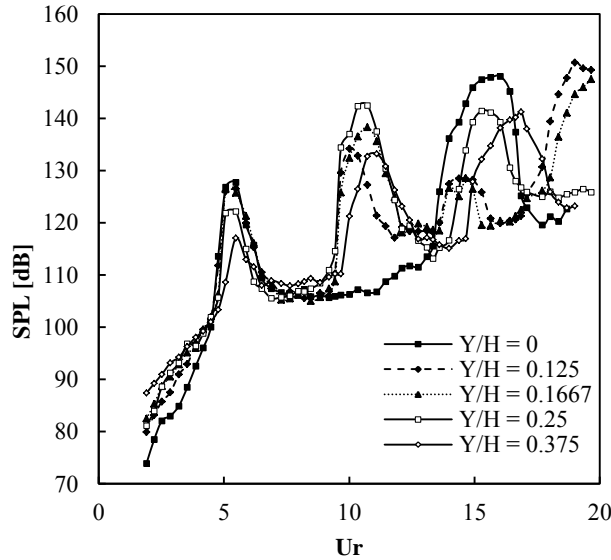


Figure 10: Comparison of the sound pressure levels at different vertical cylinder's locations, $D= 12.7$ mm.

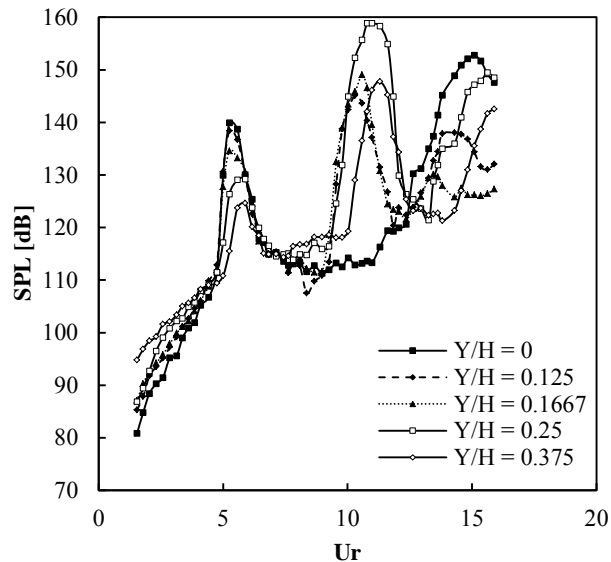


Figure 11: Comparison of the sound pressure levels at different vertical cylinder's locations, $D= 15.7$ mm.

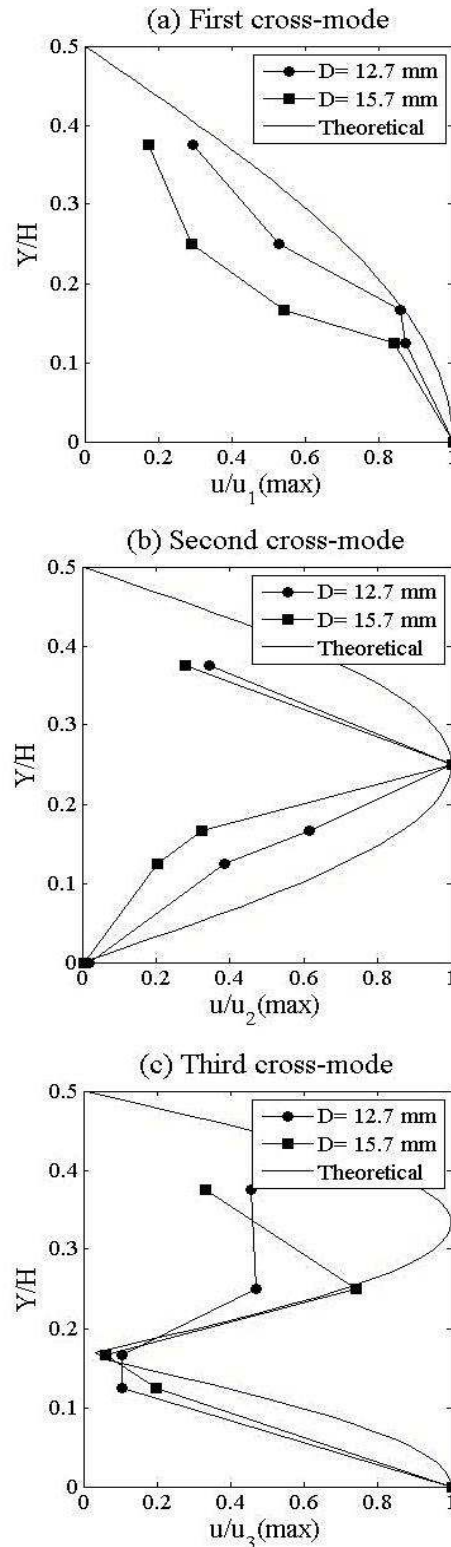


Figure 12: Distribution of the ratio of acoustic particle velocity to the maximum value of acoustic particle velocity along the duct height for (a) first, (b) second, (c) third cross-modes. The theoretical normalized distribution of the acoustic particle velocity is shown in each case.

It is observed from Figure (12) that the distribution seems to follow the theoretical sinusoidal distribution of the acoustic particle velocity. This indicates that the excitation mechanism depends, to some extent, on the acoustic particle velocity distribution rather than the acoustic pressure distribution. It is also worth to mention that the frequency values of each excited acoustic cross-mode were not constant for all the tested cases. Tables (1) and (2) show the acoustic resonance frequencies for the first three cross-modes for a cylinder diameter of 12.7 and 15.7 mm, respectively. The variation in the resonance frequencies can be explained by the fact that the existence of the cylinder changes the path of the oscillating fluid particles, and hence the frequency will differ for different cylinder diameters. However, this effect is more pronounced for the third acoustic cross-mode, which could be the result of an added acoustic damping. Caughey and O’Kelly [21] observed similar trend for a linear dynamic system and reported that the highest natural frequency decreases because of the added damping effect.

Table 1: Frequency values of each excited acoustic cross-mode, D=12.7 mm.

Y/H	First cross-mode (Hz)	Second cross-mode (Hz)	Third cross-mode (Hz)
0	678	(not excited)	1884
0.125	682	1327	1921
0.1667	679	1323	(not excited)
0.25	681	1326	1886
0.375	681	1324	1914

Table 2: Frequency values of each excited acoustic cross-mode, D=15.7 mm.

Y/H	First cross-mode (Hz)	Second cross-mode (Hz)	Third cross-mode (Hz)
0	676	(not excited)	1812
0.125	676	1319	1855
0.1667	676	1321	(not excited)
0.25	677	1319	1826
0.375	679	1327	1846

Finally, the Strouhal number values were investigated for different cylinder’s locations. Rao et al. [22] investigated the characteristic of the wake of a cylinder close to solid boundary. They have shown that the average Strouhal number value varies with the gap distance. This Strouhal number variation affects the relationship between the frequency and flow velocity and thus may change the onset of acoustic resonance. Figure (13) shows the variation of Strouhal number with the cylinder’s locations. As the cylinder moves

closer to the wall, the average Strouhal number decreases due to the interference between the wake of the cylinder and the duct’s wall. Therefore, the onset of acoustic resonance for such cases occurs at higher flow velocities, as can be seen in Figures (10) and (11).

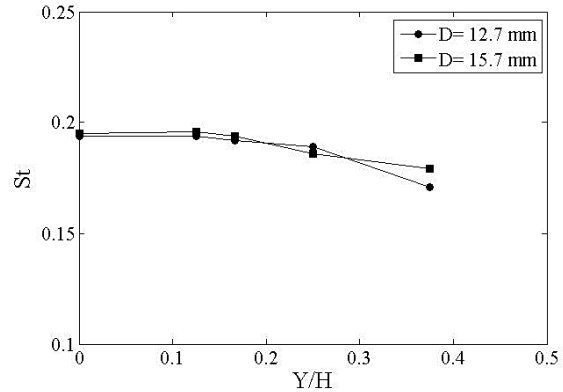


Figure 13: Average Strouhal number versus the cylinder’s location.

6. CONCLUSIONS

The effect of cylinder location on the excitation mechanism of the flow-excited acoustic resonance is presented in this work. It has been found that the cylinder’s location affects the level of acoustic excitation for each cross-mode. It is observed that when the cylinder is placed at the acoustic pressure node of a certain cross-mode, which is the acoustic particle velocity anti-node, the excitation of this particular cross-mode is dominant. It is also observed that as the cylinder moves away from the acoustic particle velocity anti-node of a certain cross-mode, the levels of the generated acoustic pressure decrease. This variation in the excitation levels seems to follow the theoretical sinusoidal distribution of the acoustic particle velocity which indicates that the excitation mechanism depends on the acoustic particle velocity distribution rather than the acoustic pressure distribution. The Strouhal number is calculated for different cylinder locations and is shown to decrease as the cylinder moves away from the duct’s centerline. This, in turn, shifts the onset of acoustic resonance to occur at higher flow velocities for these cases.

ACKNOWLEDGEMENT

The authors would like to acknowledge the financial support provided by the Natural Sciences and Engineering Research Council of Canada (NSERC). The authors also appreciate the help of Mr. Salim El-Bouzidi for providing the French abstract.

REFERENCES

1. Blevins, R.D., 2001. *Flow-Induced Vibration*, second ed. Krieger Publishing Company, USA.
2. Rayleigh, Lord J., 1879. Acoustical Observation II. *Philosophical magazine*, Vol. 7, issue 42, pp. 149-162.
3. Benard, W., 1908. Formation of centers of circulation behind a moving obstacle (In French), *Comptes Rendus Academie des Science*, 147, pp. 970-972, (translated by Zdravkovich 1997).
4. Relf, E. F., 1921. On the sound emitted wires of circular section when exposed to air current. *Philosophical magazine*, Vol. 42, issue 247, pp. 173-176.
5. Zdravkovich, M.M., 1997. *Flow around Circular Cylinders*. Vol. 1: Fundamentals, Oxford University press.
6. Mohany, A., Ziada, S., 2011. Measurements of the dynamic lift force acting on a circular cylinder in cross-flow and exposed to acoustic resonance. *Journal of Fluids and Structures*, Vol. 27, pp. 1149–1164.
7. Blevins, R.D., Bressler, M.M., 1993. Experiments on acoustic resonance in heat exchanger tube bundles. *Journal of Sound and Vibration*, 164(3), pp. 503-533.
8. Ziada, S., Oengoren, A. and Buhlmann, E. T., 1989. On acoustical resonance in tube arrays: Part I. Experiments, *Journal of Fluids and Structures*, 3(3), pp. 293-314.
9. Ziada, S., and Oengoren, A., 1990, Flow-induced acoustical resonance of in-line tube bundles, *Sulzer Technical Review*, 1, pp. 45-47.
10. Ziada, S. and Oengoren, A., 1992, Vorticity shedding and acoustic resonance in an in-line tube bundle part I: Vorticity shedding. *Journal of Fluids and structures*, 6(3), pp. 271-292.
11. Oengoren, A. and Ziada, S., 1992, Vorticity shedding and acoustic resonance in an in-line tube bundle part II: Acoustic Resonance. *Journal of Fluids and structures*, 6(3), pp. 293-302.
12. Eisinger, F.L., Francis, J. T., and Sullivan, R.E., 1996, Prediction of acoustic vibration in steam generator and heat exchanger tube banks. *ASME Journal of Pressure Vessel Technol.*, vol. 118, pp. 221-236.
13. Eisinger, F.L., and Sullivan, R.E., 2003, Suppression of acoustic waves in steam generator and heat exchanger tube banks. *ASME Journal of Pressure Vessel Technol.*, vol. 125, pp. 221-227.
14. Feenstra, P.A., Weaver, D.S. and Eisinger, F.L., 2006. A study of acoustic resonance in a staggered tube array. *ASME Journal of Pressure Vessel Technol.*, vol. 128, pp. 533-540.
15. Weaver, D. S., 1993, Vortex shedding and acoustic resonance in heat exchanger tube arrays. In: *Technology for the '90s* (ed MK Au-Yang), AMSE, New York, pp. 776-810.
16. Chen, S. S., 1987. *Flow-induced vibration of circular cylindrical structures*. Springer-Verlag, Berlin.
17. Zdravkovich, M.M., Nuttall, J. A., 1974. On the elimination of Aerodynamic Noise in a Staggered Tube Bank. *Journal of Sound and Vibration*, 34(2), pp. 173-177.
18. Kinsler, L. E., Frey, A. R., Coppens, A. B., Sanders, J. V., 2000. *Fundamentals of Acoustic*. 4th ed. John Wiley and Sons, Inc. pp. 47-51.
19. Mohany A., Ziada S., 2009. Numerical Simulation of the Flow Sound Interaction Mechanisms of a Single and two Tandem Cylinders in Cross-Flow. *ASME Journal of Pressure Vessel Technology*, vol. 131, p. 031306;
20. Lienhard, J. H., 1966. Synopsis of lift, drag, and vortex frequency data for rigid circular cylinder. Washington State University, College of Engineering, Research Division, Bulletin 300.
21. Caughey T. K., O'Kelly M. E. J., 1961. Effect of Damping on the Natural Frequencies of Linear Dynamic Systems. *Journal of the Acoustical Society of America*. Vol. 33, Issue 11, pp. 1458-1461.
22. Rao A., Thompson, M. C., Leweke, M. C., Hourigan, K., 2013. The flow past a circular cylinder translating at different heights above a wall. *Journal of Fluids and Structures*. Vol. 41, pp. 9–21.

Better testing... better products.

The Blachford Acoustics Laboratory Bringing you superior acoustical products from the most advanced testing facilities available.



Our newest resource offers an unprecedented means of better understanding acoustical make-up and the impact of noise sources. The result? Better differentiation and value-added products for our customers.

Blachford Acoustics Laboratory features

- Hemi-anechoic room and dynamometer for testing heavy trucks and large vehicles or machines.
- Reverberation room for the testing of acoustical materials and components in one place.
- Jury room for sound quality development.



Blachford acoustical products

- Design and production of simple and complex laminates in various shapes, thicknesses and weights.
- Provide customers with everything from custom-engineered rolls and diecuts to molded and cast-in-place materials.

Blachford QS 9000
REGISTERED



www.blachford.com | Ontario 905.823.3200 | Illinois 630.231.8300





Cadna R[®]
Prediction of
Noise Levels inside Rooms

New: Interior Noise calculation with CadnaR



- Intuitive handling
- Efficient workflow
- Unique result display
- Detailed documentation
- Excellent support

❖ Intuitive Handling

The software is clearly arranged to enable you to build models and make simple calculations easily. At the same time you benefit from the sophisticated input possibilities as your analysis becomes more complex. Focus your time on the project and not on the software. All input and analysis features are easy and intuitive to handle.

❖ Efficient Workflow

Change your view from 2D to 3D within a second. Multiply the modeling speed by using various shortcuts and automation techniques. Many time-saving acceleration procedures enable fast calculations of your projects.

❖ Modern Analysis

CadnaR uses scientific and highly efficient calculation methods. Techniques like scenario analysis, grid arithmetic or the display of results within a 3D-grid enhance your analysis and support you during the whole planning and assessment process.

❖ Further informations at www.Datakustik.com



Distributed (USA/Canada) by:
Scantek, Inc.
Sound and Vibration Instrumentation
and Engineering

6430c Dobbin Rd Columbia, MD 21045
410-290-7726, 410-290-9167 fax
301-910-2813 cell PeppinR@ScantekInc.com
www.ScantekInc.com

EDITORIAL BOARD / COMITÉ ÉDITORIAL

Hearing Conservation - Préservation de l'ouïe

Alberto Behar (416) 265-1816 albehar31@gmail.com
Ryerson University

Musical Acoustics / Electroacoustics - Acoustique musicale / électroacoustique

Annabel J Cohen acohen@upei.ca
University of P.E.I.

Signal Processing / Numerical Methods - Traitement des signaux / Méthodes numériques

Tiago H. Falk (514) 228-7022 falk@emt.inrs.ca
Institut National de la Recherche Scientifique, Centre Énergie, Matériaux, Télécom-
munications (INRS-EMT)

Aeroacoustics - Aéroacoustique

Anant Grewal (613) 991-5465 anant.grewal@nrc-cnrc.gc.ca
National Research Council

Physiological Acoustics - Physio-acoustique

Robert Harrison (416) 813-6535 rvh@sickkids.ca
Hospital for Sick Children, Toronto

Underwater Acoustics - Acoustique sous-marine

Garry J. Heard 902-426-3100 x310 garry.heard@drdc-rddc.gc.ca
Defence R-D Canada Atlantic Research Centre

Psychological Acoustics - Psycho-acoustique

Jeffery A. Jones jjones@wlu.ca
Wilfrid Laurier University

Consulting - Consultation

Tim Kelsall 905-403-3932 tkelsall@hatch.ca
Hatch

Architectural Acoustics - Acoustique architecturale

Jean-François Latour (514) 393-8000 jean-francois.latour@snclavalin.com
SNC-Lavalin

Shocks / Vibrations - Chocs / Vibrations

Pierre Marcotte marcotte.pierre@irsst.qc.ca
IRSST

Hearing Sciences - Sciences de l'audition

Kathleen Pichora Fuller (905) 828-3865 k.pichora.fuller@utoronto.ca
University of Toronto

Speech Sciences - Sciences de la parole

Linda Polka 514-398-7235 linda.polka@mcgill.ca
McGill University

Physical Acoustics / Ultrasounds - Acoustique physique / Ultrasons

Werner Richarz wricharz@echologics.com

Bio-Acoustics - Bio-acoustique

Jahan Tavakkoli (416) 979-5000 jtavakkoli@ryerson.ca
Ryerson University

Engineering Acoustics/Noise Control - Génie Acoustique/Contrôle du bruit

Vacant

Simplicity

NEW!

SoundExpert™ LxT

- An All-In-One, Class 1 Sound Level Meter
- A Product Development Tool
- A Complete Noise Monitoring Kit (Option)



Total Customer Satisfaction
LARSON DAVIS
A PCB GROUP COMPANY

Dalimar
instruments
A PCB GROUP COMPANY

Tel: 450-424-0033 • Fax: 450-424-0030
Website: www.dalimar.ca • Email: info@dalimar.ca



www.LarsonDavis.com/SoundExpertLxT